Chapter 1.1

Hyperspectral and multispectral imaging: setting the scene

José Manuel Amigo*
Professor, Ikerbasque, Basque Foundation for Science; Department of Analytical Chemistry, University of the Basque Country, Spain; Chemometrics and Analytical Technologies, Department of Food Science, University of Copenhagen, Denmark
**Corresponding author. e-mail: jmar@life.ku.dk*

1. Images: basic concepts, spatial resolution, and spectral information

It might be a bit odd to start a book about hyperspectral imaging (HSI) and multispectral imaging (MSI) by defining what an "image" is. Nevertheless, I found it very appropriated, since nowadays the literature is full of surnames or forenames adopted depending on the type of images we are talking about. Terms like chemical imaging, confocal imaging, HSI, MSI, satellite imaging, microscope imaging, etc., are filling the papers, depending on the type of device used for acquiring the image or sometimes the use we want to give to the image. Thus, according to the *Oxford Dictionary*, an image is the representation of the external form of a person or thing in art. It is also a visible impression obtained by a camera, telescope, microscope, or other device, or displayed on a computer video screen [1]. For our purpose, let us say that an image is a bidimensional representation of a surface produced by any device that has the ability to obtain information in an X−Y direction of the surface in a correlated manner.

1.1 Spatial resolution

From my point of view, the most appropriate concept of image is the mathematical one, "an image is a point or set formed by mapping from another point or set." That is, to create an image, you need, at least, two-point sets. Putting together both definitions, it is clear that these two-point sets must be

Hyperspectral Imaging. https://doi.org/10.1016/B978-0-444-63977-6.00001-8

somehow spatially correlated, providing us the indirect definition of pixel, the second most used term in imaging. A pixel is the spatial subdivision of images. They are unique pieces of information that are, as well, spatially correlated. In other words, a pixel is affected by the surrounding pixels in such a way that the information contained in one of them depends on the information that the surrounding pixels contain (i.e., neighbors).

A clear distinction must be made between the total amount of pixels and the size of that pixel with respect to the full image that it is being measured. If an image is the spatial representation of a surface, and that image is divided into pixels, the term spatial resolution comes up. According to the international standards, the spatial resolution of an image is the total amount of pixels in which an image is divided. A basic example is that if an image contains X pixels in the row direction and Y pixels in the column direction, the image has a spatial resolution of $X \times Y$ pixels. Even accepting this as a common practice, it must be stressed that this definition is incomplete. The spatial resolution must be always measured in relative terms of distance. For instance, let us give the example of having a camera that is 10×10 pixels. If that camera is taking the picture of a 1×1 m, the real spatial resolution should be said to be 0.01 m^2; while if the same camera is taking a picture of 0.5×0.5 m, the spatial resolution should be said to be 0.0025 m^2. This will directly address the need of setting the area of the surface information that every pixel contains.

1.2 Spectral information: types of images

There are different ways of classifying images. One of the most adequate ways is considering the amount of information that a pixel can contain. The information can come from a simple difference in intensities with respect to a reference, generating one single channel of information per pixel (e.g., scanning electron microscopy (SEM) images). Nevertheless, it is common nowadays to find images that contain more channels of information for each pixel. These are the color-space images, the multispectral images, and the hyperspectral images.

1.2.1 Single channel images

Images for which there is only a single value of intensity for each pixel are called monochannel or single channel images. The values that each pixel can have vary depending of the type of device taking the image, and they are normally ranging between certain limits. For instance, Fig. 1 shows one single channel image of yogurt obtained with confocal laser scanning microscopy (CLSM) (see Ref. [2] for further details). Single channel images can be extracted from any image device by choosing one channel of spectral information or by using a device that only gives one point of information per pixel (e.g., CLSM, SEM, atomic force microscopy (AFM), etc.).

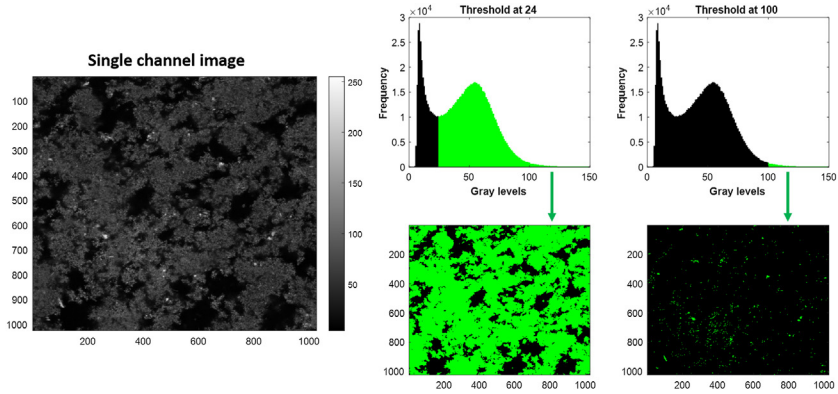

FIGURE 1 Confocal laser scanning microscopy image of a yogurt sample. The image is one of the images used in Ref. [2]. The right part of the figure shows the histogram of the grayscale values and the result of applying two different threshold values (24 for protein and 100 for microparticulated whey protein).

There are many ways of representing a single channel image by using different color maps. The most popular one is the grayscale color map in which the intensity value corresponds to a specific value of the grayscale (denoted with the corresponding color bar in Fig. 1). Normally, the spatial resolution of these devices trends to be considerably good, arising to microscope scale. The main drawback is normally the lack of chemical information, since all the information relies on one single value. Therefore, one of the most common methods to analyze these images is the direct application of thresholds, grouping the pixels in groups with similar value of pixel (ref digital image). Coming back to the example in Fig. 1, two different thresholds applied to the same picture give two different responses. In this case, the threshold around 24 gives an account of total protein content, while the threshold around 100 gives an account of microparticulated whey protein [2].

1.2.2 Color-space images

Color-space images are the images that try to mimic the human vision. They are composed normally by three channels of spectral information, the red (around 700 nm), green (around 550 nm), and blue (around 450 nm), that combined are able to recreate real colors in what is known as the RGB color space (image denoted as real color in Fig. 2) [3]. It is important to remark that the RGB is not the only color space that is used in this type of images. There are many ways of coding the color in other color spaces (like the hue−saturation−value color-space or the luminosity-Red to Green-Blue gradient (L*a*b*), among others [3]) (Fig. 2).

Color-space images are known for many years, and the technology for obtaining them is continuously advancing. Defining that technology is out of

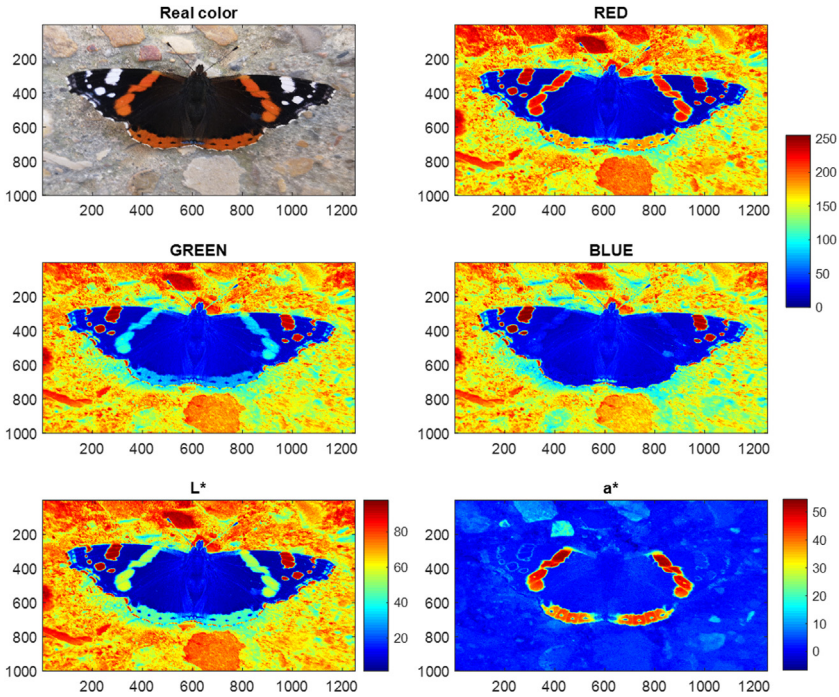

FIGURE 2 Real color picture in RGB color space of a butterfly, and representation of the red, green, and blue monochannels using the color map displayed in the right part of the figure. The two images in the bottom are the transformed image in L*a*b* color space.

this book chapter. However, it is important to remark that these images have normally a high spatial resolution, and once the illumination and the focal distance is controlled, they can be extremely powerful devices with limited chemical information. For instance, a flatbed scanner in the RGB mode can be an extraordinary analytical tool for specific cases since they have a high spatial resolution, the light income is constant and the focal distance is normally fixed [4–6].

1.2.3 Multiband images

Multiband or multispectral images are those that capture individual images at specific wave numbers or wavelengths, frequently taken by specific filters or LEDs, across the electromagnetic spectrum (normally the visible (VIS) and near-infrared (NIR) regions [7]. Multispectral images can be considered as special case of hyperspectral images in which the wavelength range collected cannot be considered as continuous. That is, instead a continuous measurement between a certain wavelength range, the multispectral images contain information in discrete and specific wavelengths. Fig. 3 shows an example of a

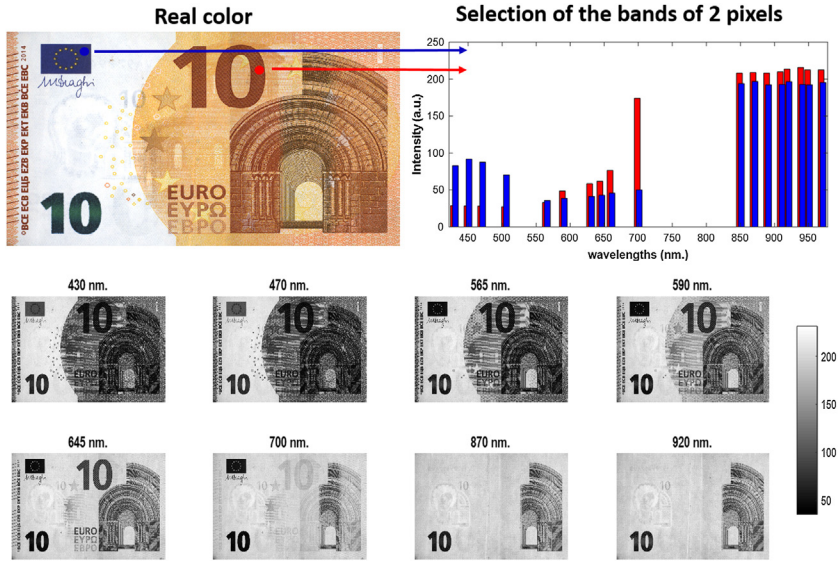

FIGURE 3 Multispectral image taken to a 10 euros paper note (top left). The top right part shows the intensities of the 19 different wavelengths for two pixels. The bottom part shows different single channel pictures extracted for eight channels.

10 euros paper note that has been measured at 18 different wavelengths. That is, every single pixel contains the specific information collected at 18 different wavelengths. As it can be observed in the figure, when the sample is irradiated with light at different wavelengths, specific information is obtained. Each individual image can be considered as a single channel image. Therefore, it is mandatory to place the corresponding values of the color intensities obtained in each individual image.

As we will see in further chapters, the fact of differentiating MSI from HSI is due to the different treatment that must be given to the images. The spectra obtained with MSI cannot be considered spectra, since normally the spectral signatures are measured at nonequidistant discrete wavelengths. It was applied in remote sensing, and it was the precursor of the hyperspectral images. A good example of MSI applied in remote sensing is the well-known Landsat satellite [8].

1.2.4 Hyperspectral images

Hyperspectral images are the images in which one continuous spectrum is measured for each pixel [9]. Normally, the spectral resolution is given in nanometers or wave numbers (Fig. 4).

Hyperspectral images can be obtained from many different electromagnetic measurements. The most popular are visible (VIS), NIR, middle infrared

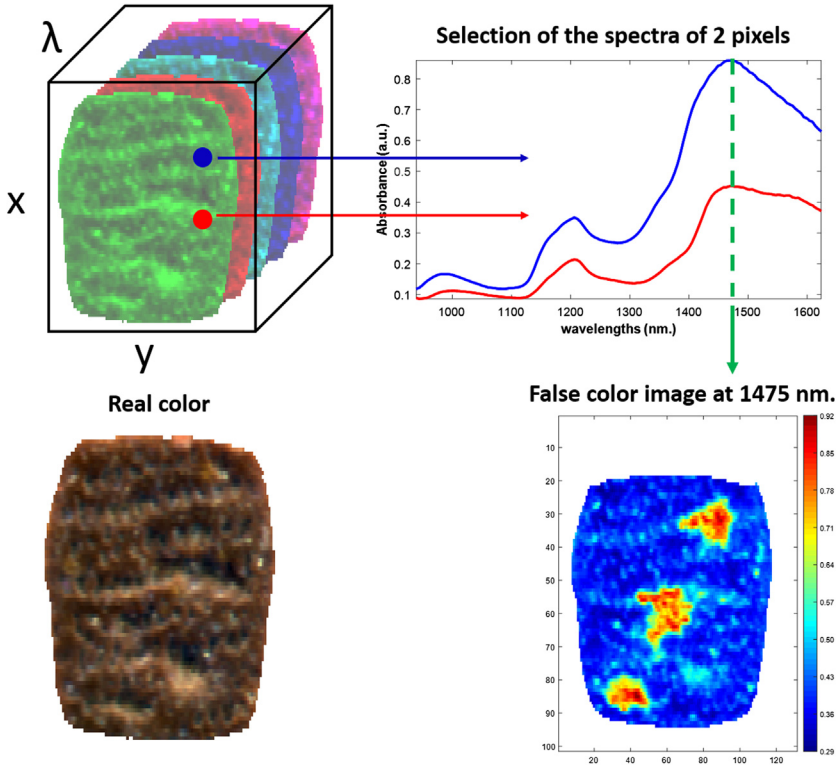

FIGURE 4 Representation of the image of a cookie measured with a hyperspectral camera in the wavelength range of 940−1600 nm (near infrared, NIR) with a spectral resolution of 4 nm. The spectra obtained in two pixels are shown and the false color image (single channel image) obtained at 1475 nm. The single channel image selected highlighted three areas of the cookie where water was intentionally added. This water is invisible in the VIS region (nothing can be appreciated in the real color picture). Nevertheless, water is one of the main elements that can be spotted in NIR.

(MIR), and Raman spectroscopy. Nevertheless, there are many other types of HSI that are gaining popularity like confocal laser microscopy scanners that are able to measure the complete emission spectrum at certain excitation wavelength for each pixel, Terahertz spectroscopy, X-ray spectroscopy, 3D ultrasound imaging, or even magnetic resonance.

Hyperspectral images are the only type of images where we can talk about spectral resolution (also known as radiometric resolution in remote sensing field). The spectral resolution is defined as the interval or separation (gap) between different wavelengths measured in a specific wavelength range. Obviously, the more bands (or spectral channels) acquired in a smaller wavelength range, the higher the spectral resolution will be.

2. Data mining: chemometrics

2.1 Structure of a hyperspectral image

A hyperspectral or multispectral image can be visualized as a hypercube of data (Figs. 3 and 4). The hypercube is defined by three dimensions: Two spatial (X and Y) and one spectral (λ) [9]. The mathematical notation will be, then, a hypercube **D** will have dimensions ($X \times Y \times \lambda$) [9]. This structure contains all the chemical information related to the surface measured. That is, hyperspectral data cubes are normally multicomponent systems. The pixels measured seldom contain selective wavelengths for a specific component since they trend to contain mixed information of more than one component. Moreover, it also contains artifacts like the spectral noise, spatial interferences, and redundant information. Therefore, there is a strong need to extract the desired information and get rid of the noise and further artifacts. As we will see further in the book, there is a plethora of algorithms that are able to extract the desired information from the data cube, and there are more and more coming due to the generation of faster computers and more reliable sensors.

2.2 Chemometrics

It can be said without mistake that one of the major reasons for the expansion of HSI and MSI is the integration of data mining to extract the relevant information from the data cube in a multivariate fashion. Most of the information gathered with HSI and MSI can be considered as chemical information. Therefore, it is also called chemometrics. Chemometrics is basically data mining applied to chemical information by using mathematical, statistical, and data analysis methods to achieve objective data evaluation by extracting the most important information from related and unrelated collections of chemical data by using mathematical and statistic tools [10].

The main aim of chemometrics is to provide a final image where selective information for a specific component can be found (in terms of concentration/quantitative or presence/qualitative). Nevertheless, one of the major problems of chemometrics is that sometimes it becomes cumbersome to know which method to apply in each situation [9]. This will be unraveled and defined during the book. Fig. 5 gives an account of the major building blocks of data mining/chemometrics application in HSI and MSI. This flowchart is merely a guidance, and the methods included there are not exclusive for the building blocks. Also, the path to follow is strongly dependent of the type of analysis and the final target.

The main building blocks in the analysis of HSI and MSI images (Fig. 5) are preprocessing, pattern recognition/exploration, resolution/spectral unmixing, segmentation, regression, classification, and image processing [9]. Each one of them aims at different purposes:

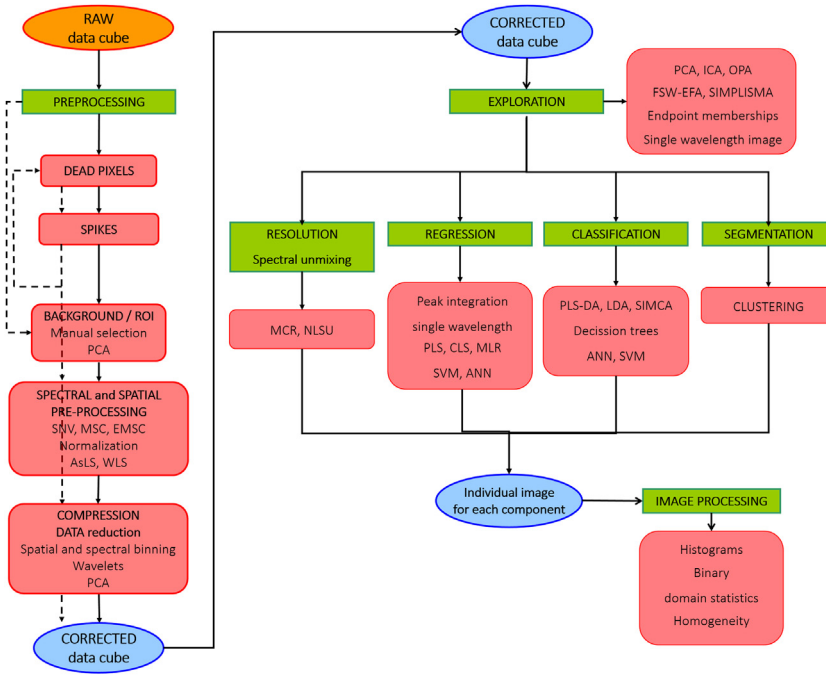

FIGURE 5 Comprehensive flowchart of the analysis of hyperspectral and multispectral images. *ANN*, artificial neural networks; *AsLS*, asymmetric least squares; *CLS*, classical least squares; *EMSC*, extended multiplicative scatter correction; *FSW-EFA*; fixed size window-evolving factor analysis; *ICA*, independent component analysis; *LDA*, linear discriminant analysis; *MCR*, multivariate curve resolution; *MLR*, multiple linear regression; *MSC*, multiplicative scatter correction; *NLSU*, nonlinear spectral unmixing; *OPA*, orthogonal projection approaches; *PCA*, principal component analysis; *PLS-DA*, partial least squares-discriminant analysis; *PLS*, partial least squares; *SIMCA*, soft independent modeling of class analogy; *SIMPLISMA*, simple-to-use interactive self-modeling mixture analysis; *SNV*, standard normal variate; *SVM*, support vectors machine; *WLS*, weighted least squares. *Partially extracted and modified from J.M. Amigo, H. Babamoradi, S. Elcoroaristizabal, Hyperspectral image analysis. A tutorial, Analytica Chimica Acta 896 (2015) 34–51. doi:10.1016/j.aca.2015.09.030. with permission of Elsevier.*

2.2.1 Preprocessing

Sometimes this is a previous step that does not have the deserved importance, and, nevertheless, it is the main responsible for obtaining optimal results when any multivariate data model is applied afterward. The presence of erroneous or missed data values (e.g., dead pixels [7]), noninformative background, or extreme outliers; or the presence of spatial and spectral artifact (e.g., scattering or atmospheric influence) are aspects that must be considered way before or even during the modeling part. There are many methods for minimizing artifacts in our data or to highlight information on it (in both spectral and

spatial directions). And, luckily, there are many algorithms that can help in this quest. Nevertheless, the decision of the proper preprocessing method is not sometimes straightforward, and normally is based in the combination of different methods to achieve a preprocessed data cube that, still, needs to be processed properly.

2.2.2 Pattern recognition/exploration

Pattern recognition is, among the building blocks of Fig. 5, the only ones that can be purely denoted as not supervised (or unsupervised). They do not need a previous step of calibration (training), neither a decision step (e.g., number of components needed) in order to find hidden patterns in the data. The purpose of the unsupervised methods is to identify relationships between pixels, without any prior knowledge of classes or groups. They are used to give a first overview of the main sources of variance (variability) in the images. Among them, the most common method is principal component analysis (PCA). PCA is useful in order to elucidate the complex nature of HSI and MSI multicomponent systems by using mapping and displaying techniques [9,11].

2.2.3 Segmentation

Segmentation methods compile all the clustering methodologies and dendrograms [12]. They divide the pixels in different groups considering their spectral similarities and dissimilarities. And even being unsupervised methods (no training step needed), there is a step in which a decision should be made. In the case of clustering, it is essential to guess the final number of clusters, and in dendrograms, a threshold must be set in order to group the pixels. Even though segmentation methods group the pixels according to their similarity, they cannot be considered as classification methods, since no training step is used.

2.2.4 Curve resolution methods/spectral unmixing

Curve resolution or spectral unmixing methods aim at resolving mixtures that each individual pixel might contain, given the correct number of constituents [13,14]. The final result is a set of selective images for each constituent and their pure spectral profile. The main difference with explorative methods like PCA is that curve resolution methods do not aim at studying the main sources of variation in the data, but at giving an account of the hidden physicochemical behavior of each constituent in each pixel. A big debate could be stablished concerning the nature of curve resolution methods. In some aspects, they behave as unsupervised methods. Nevertheless, many of the occasions they rely in giving good initial estimations and proper spectral and spatial constraints to obtain a suitable response.

2.2.5 Regression and classification

Calculating the concentration of several compounds in an image (regression) and, specially, the classification of elements in different well-defined categories (classification) is one of the major targets in HSI and MSI analysis. Regression and classification methods are pure supervised methods, since a robust and reliable set of samples of well-known concentration or well-known category is needed for the essential step of training of the model (calibration step). Once the training is perfectly performed, the properties or the classes are predicted in new images in a pixel-by-pixel manner [15]. Many algorithms for linear or nonlinear training models like partial least squares (PLS), multilinear regression, support vectors machine, or artificial neural networks can be found in regression and their adaptation for classification purposes (e.g., PLS-discriminant analysis). Moreover, many algorithms can be found being specifically designed for a purpose, like the single class approach that SIMCA (soft independent modeling of class analogy) offers [16]. Being supervised methods, the core of their reliability depends on the *mandatory validation* step. Validation (internal cross-validation or external validation) is the only tool able to give a real account of the ability of the model to predict.

2.2.6 Image processing

Once one selective image for each individual constituent is achieved, the final aim might be to analyze the distribution, amount, shape of those constituents in the surface measured. This is directly linked to the well-known digital imaging processing methodologies [3]. There is, again, a plethora of algorithms that can be used for many different purposes. It is not the aim of this book chapter to focus on those methods. Therefore, we encourage the readers to read the provided references to have a better account of them [3].

3. Growing the number of application fields of HSI and MSI

The evolution in HSI and MSI cameras in the market has grown exponentially since the first works in remote sensing were published in the late 1970s, beginning of 1980s. The first scientific instrument capable of measuring MSI images was developed by Goetz et al. [17]. It was called the Shuttle Multispectral Infrared Radiometer (SMIRR), and it was placed in the second flight of the space shuttle in 1981 [17,18]. SMIRR was able to measure 10 narrow bands, and the main purpose was the identification of minerals in the surface of the planet. Seeing the excellent results, Goetz et al. proposed the creation of what it would be the first HSI camera, the Airbone Imaging Spectrometer (AIS) [19]. AIS was the first HSI camera that was able to collect 128 spectral bands in the range of 1200−2400 nm with a spectral resolution of 9.6 nm. The detector was able to collect a line of 32 pixels moving as a scanner (what is commonly known line mapping or push broom systems [19]).

From this point on, the technological advances in HSI and MSI have generated the eruption of the application fields within the area of remote sensing [20]. These technological advances are due to the rapid increasing in the sensing technology, higher computational capability, more robust and versatile instruments that can be adapted in different scenarios, and, of course, improvement in the data mining algorithms for processing the overwhelming amount of data that were being generated [21–23]. Airborne and satellite imaging opened the applications in the mineralogy [17], oceanography [24], environmental monitoring and water resources management [25], vegetation [23,26], or precision agriculture [27]. Moreover, soon the scientific knowledge generated to create cameras working on the visible and NIR spectral range was also applied to other spectral radiations like MIR, Raman, nuclear magnetic resonance (NMR), fluorescence, X-ray, or even Terahertz spectroscopy, exponentially increasing the amount of applications of HSI and MSI cameras [28].

Another of the major breakthroughs was produced when the HSI and MSI started to be adapted in more controlled environments. Normally, there is a "from minor to major" path in sciences. That is, new devices are developed in the laboratories, and then the devices go out of the laboratory environment. With HSI and MSI, the evolution was "from major to minor," from satellites scanning the planet to the laboratory. Fields like biochemistry [29], food processing [27,30–34], pharmaceutical research and processing [12,35–38], forensic investigations [39,40], artwork and cultural heritage [41,42], medical research [43], recycling [9,44,45], among other areas started to use the same cameras as in remote sensing but adapted to their particular problem.

All in all, and to finish this introductory chapter, I can certify that even though HSI and MSI are a science that is around 50 years old, it is still new and exciting. And there is an exciting and challenging future ahead of us, where faster and more reliable hyperspectral cameras will be developed and, consequently, the data analysis technology to analyze them.

References

[1] O. university Press, Oxford dictionary, (n.d.). https://www.oxforddictionaries.com/.

[2] I.C.I.C. Torres, J.M. Amigo Rubio, R. Ipsen, J.M. Amigo, R. Ipsen, Using fractal image analysis to characterize microstructure of low-fat stirred yoghurt manufactured with microparticulated whey protein, Journal of Food Engineering 109 (2012) 721–729, https://doi.org/10.1016/j.jfoodeng.2011.11.016.

[3] R.C. Gonzalez, R.E. Woods, S.L. Eddins, Digital Image Processing Using Matlab, 2004, https://doi.org/10.1117/1.3115362.

[4] M. Vidal, J.M.M. Amigo, R. Bro, F. van den Berg, M. Ostra, C. Ubide, Image analysis for maintenance of coating quality in nickel electroplating baths – real time control, Analytica Chimica Acta 706 (2011) 1–7, https://doi.org/10.1016/j.aca.2011.08.007.

[5] L. de Moura França, J.M. Amigo, C. Cairós, M. Bautista, M.F. Pimentel, J. Manuel Amigo, C. Cair os, M. Bautista, M. Fernanda Pimentel, Evaluation and assessment of homogeneity in images. Part 1: unique homogeneity percentage for binary images, Chemometrics and Intelligent Laboratory Systems 171 (2017), https://doi.org/10.1016/j.chemolab.2017.10.002.

[6] N.C. da Silva, L. de Moura França, J.M. Amigo, M. Bautista, M.F. Pimentel, Evaluation and assessment of homogeneity in images. Part 2: homogeneity assessment on single channel non-binary images. Blending end-point detection as example, Chemometrics and Intelligent Laboratory Systems 180 (2018), https://doi.org/10.1016/j.chemolab.2018.06.011.

[7] M. Vidal, J.M. Amigo, Pre-processing of hyperspectral images. Essential steps before image analysis, Chemometrics and Intelligent Laboratory Systems 117 (2012) 138−148, https://doi.org/10.1016/j.chemolab.2012.05.009.

[8] NASA, Landsat Science, (n.d.). https://www.oxforddictionaries.com/.

[9] J.M. Amigo, H. Babamoradi, S. Elcoroaristizabal, Hyperspectral image analysis. A tutorial, Analytica Chimica Acta 896 (2015) 34−51, https://doi.org/10.1016/j.aca.2015.09.030.

[10] D.L. Massart, B.G.M. Vandeginste, J.M.C. Buydens, S. de Jong, P.J. Lewi, J. Smeyers-Verberke, L.M.C. Buydens, S. De Jong, J. Smeyers-Verbeke, Handbook of Chemometrics and Qualimetrics, 1997. https://doi.org/10.1016/S0922-3487(97)80056-1.

[11] A.K. Smilde, R. Bro, Principal component analysis (tutorial review), Analytical Methods 6 (2014) 2812−2831. https://doi.org/10.1039/c3ay41907j.

[12] J.M. Amigo, J. Cruz, M. Bautista, S. Maspoch, J. Coello, M. Blanco, Study of pharmaceutical samples by NIR chemical-image and multivariate analysis, Trends in Analytical Chemistry 27 (2008). https://doi.org/10.1016/j.trac.2008.05.010.

[13] F. Franch-Lage, J.M. Amigo, E. Skibsted, S. Maspoch, J. Coello, Fast assessment of the surface distribution of API and excipients in tablets using NIR-hyperspectral imaging, International Journal of Pharmaceutics 411 (2011) 27−35. https://doi.org/10.1016/j.ijpharm.2011.03.012.

[14] A. de Juan, R. Tauler, Multivariate curve resolution (MCR) from 2000: progress in concepts and applications, Critical Reviews in Analytical Chemistry 36 (2006) 163−176. https://doi.org/10.1080/10408340600970005.

[15] C. Ravn, E. Skibsted, R. Bro, Near-infrared chemical imaging (NIR-CI) on pharmaceutical solid dosage forms-comparing common calibration approaches, Journal of Pharmaceutical and Biomedical Analysis 48 (2008) 554−561. https://doi.org/10.1016/j.jpba.2008.07.019.

[16] S. Wold, W.J. Dunn, E. Johansson, J.W. Hogan, D.L. Stalling, J.D. Petty, T.R. Schwartz, Application of Soft Independent Method of Class Analogy (SIMCA) in Isomer Specific Analysis of Polychlorinated Biphenyls, 2009, pp. 195−234. https://doi.org/10.1021/bk-1985-0284.ch012.

[17] A.F.H. Goetz, L.C. Rowan, M.J. Kingston, Mineral identification from orbit: initial results from the shuttle multispectral infrared radiometer, Science 218 (1982) 1020−1024. https://doi.org/10.1126/science.218.4576.1020, 80-.

[18] J.S. MacDonald, S.L. Ustin, M.E. Schaepman, The contributions of Dr. Alexander F.H. Goetz to imaging spectrometry, Remote Sensing of Environment 113 (2009). https://doi.org/10.1016/j.rse.2008.10.017.

[19] G. Vane, A.F.H. Goetz, J.B. Wellman, Airborne imaging spectrometer: a new tool for remote sensing, IEEE Transactions on Geoscience and Remote Sensing GE-22 (2013) 546−549. https://doi.org/10.1109/tgrs.1984.6499168.

[20] J.B. Campbell, R.H. Wynne, Introduction to Remote Sensing, 2011.

[21] S.C. Yoon, B. Park, Hyperspectral image processing methods, in: Food Eng. Ser., 2015, pp. 81−101. https://doi.org/10.1007/978-1-4939-2836-1_4.

[22] L. Wang, C. Zhao, Hyperspectral Image Processing, 2015. https://doi.org/10.1007/978-3-662-47456-3.

[23] A. Pelizzari, R.A. Goncalves, M. Caetano, Computational Intelligence for Remote Sensing, 2008. https://doi.org/10.1007/978-3-540-79353-3.

[24] S. Martin, An Introduction to Ocean Remote Sensing, 2013. https://doi.org/10.1017/CBO9781139094368.

[25] P.S. Thenkabail, Remote Sensing Handbook: Remote Sensing of Water Resources, Disasters, and Urban Studies, 2015. https://doi.org/10.1201/b19321.

[26] P.S. Thenkabail, R.B. Smith, E. De Pauw, Hyperspectral vegetation indices and their relationships with agricultural crop characteristics, Remote Sensing of Environment (2000). https://doi.org/10.1016/S0034-4257(99)00067-X.

[27] B. Park, R. Lu, Hyperspectral Imaging Technology in Food and Agriculture, 2015. https://doi.org/10.1007/978-1-4939-2836-1.

[28] S. Delwiche, J. Qin, K. Chao, D. Chan, B.-K. Cho, M. Kim, Line-scan hyperspectral imaging techniques for food safety and quality applications, Applied Sciences 7 (2017) 125. https://doi.org/10.3390/app7020125.

[29] R. Vejarano, R. Siche, W. Tesfaye, Evaluation of biological contaminants in foods by hyperspectral imaging: a review, International Journal of Food Properties 20 (2017) 1264−1297. https://doi.org/10.1080/10942912.2017.1338729.

[30] J.M. Amigo, I. Martí, A. Gowen, Hyperspectral imaging and chemometrics. A perfect combination for the analysis of food structure, composition and quality, Data Handling in Science and Technology 28 (2013) 343−370. https://doi.org/10.1016/B978-0-444-59528-7.00009-0.

[31] S. Munera, J.M. Amigo, N. Aleixos, P. Talens, S. Cubero, J. Blasco, Potential of VIS-NIR hyperspectral imaging and chemometric methods to identify similar cultivars of nectarine, Food Control 86 (2018). https://doi.org/10.1016/j.foodcont.2017.10.037.

[32] X. Zou, J. Zhao, Nondestructive Measurement in Food and Agro-Products, 2015. https://doi.org/10.1007/978-94-017-9676-7.

[33] Y. Liu, H. Pu, D.W. Sun, Hyperspectral imaging technique for evaluating food quality and safety during various processes: a review of recent applications, Trends in Food Science & Technology 69 (2017) 25−35. https://doi.org/10.1016/j.tifs.2017.08.013.

[34] D. Wu, D.W. Sun, Advanced applications of hyperspectral imaging technology for food quality and safety analysis and assessment: a review − Part II: fundamentals, Innovative Food Science and Emerging Technologies 19 (2013) 1−14. https://doi.org/10.1016/j.ifset.2013.04.014.

[35] J.X. Wu, D. Xia, F. Van Den Berg, J.M. Amigo, T. Rades, M. Yang, J. Rantanen, A novel image analysis methodology for online monitoring of nucleation and crystal growth during solid state phase transformations, International Journal of Pharmaceutics 433 (2012) 60−70. https://doi.org/10.1016/j.ijpharm.2012.04.074.

[36] A.A. Gowen, C.P. O'Donnell, P.J. Cullen, S.E.J. Bell, Recent applications of Chemical Imaging to pharmaceutical process monitoring and quality control, European Journal of Pharmaceutics and Biopharmaceutics 69 (2008) 10−22. https://doi.org/10.1016/j.ejpb.2007.10.013.

[37] M. Khorasani, J.M. Amigo, C.C. Sun, P. Bertelsen, J. Rantanen, Near-infrared chemical imaging (NIR-CI) as a process monitoring solution for a production line of roll compaction

and tableting, European Journal of Pharmaceutics and Biopharmaceutics 93 (2015). https://doi.org/10.1016/j.ejpb.2015.04.008.

[38] A.V. Ewing, S.G. Kazarian, Recent advances in the applications of vibrational spectroscopic imaging and mapping to pharmaceutical formulations, Spectrochimica Acta Part A: Molecular and Biomolecular Spectroscopy 197 (2018) 10−29. https://doi.org/10.1016/j.saa.2017.12.055.

[39] P. Chemistry, Near promising future of near infrared hyperspectral imaging in forensic sciences, Journal of Indexing and Metrices 25 (2014) 6−9. https://doi.org/10.1255/nirn.1443.

[40] G.J. Edelman, E. Gaston, T.G. Van Leeuwen, P.J. Cullen, M.C.G. Aalders, Hyperspectral imaging for non-contact analysis of forensic traces, Forensic Science International 223 (2012) 28−39. https://doi.org/10.1016/j.forsciint.2012.09.012.

[41] C. Cucci, M. Picollo, Reflectance Spectroscopy Safeguards Cultural Assets, SPIE Newsroom, 2013. https://doi.org/10.1117/2.1201303.004721.

[42] M. Bacci, C. Cucci, A.A. Mencaglia, A.G. Mignani, Innovative sensors for environmental monitoring in museums, Sensors 8 (2008) 1984−2005. https://doi.org/10.3390/s8031984.

[43] G. Lu, B. Fei, Medical hyperspectral imaging: a review, Journal of Biomedical Optics 19 (2014) 010901. https://doi.org/10.1117/1.jbo.19.1.010901.

[44] M. Vidal, A. Gowen, J.M. Amigo, NIR hyperspectral imaging for plastics classification, Journal of Indexing and Metrices (2012). https://doi.org/10.1255/nirn.1285.

[45] D. Caballero, M. Bevilacqua, J. Amigo, Application of hyperspectral imaging and chemometrics for classifying plastics with brominated flame retardants, Journal of Spectral Imaging 8 (2019). https://doi.org/10.1255/jsi.2019.a1.